Scientific Journal for Damietta Faculty of Science **14**(2) 2024, 1-9
doi: 10.21608/sjdfs.2024.307507.1173
ISSN Print 2314-8594
ISSN Online 2314-8616

https://sjdfs.journals.ekb.eg/

Thermodynamic Parameters for the Interaction of CuCl2 with Succinic Acid in Sodium Chloride Solution using Cyclic Voltammetry

Aya A. Fouad[1], Adel Zaki El-Sonbati[1], Mostafa A. Diab[*1], Marwa R.Elsayad[2] and Esam A. Gomaa[3]

[1] Chemistry Department, Faculty of Science, Damietta University, Damietta 34517, Egypt.
[2] Ophthalmology Department, Faculty of Medicine, Mansoura University, Egypt.
[3] Chemistry Department, Faculty of Science, Mansoura University, Mansoura, Egypt.

Received: 27 July 2024 /Accepted: 31 August 2024

[*]Corresponding author's E-mail: prof.madiab@yahoo.com

Abstract

The voltammetry behavior was investigated in this work by varying the potentials of CuCl2 in the sodium chloride electrolyte. When succinic acid was present in 0.1 M NaCl-strong electrolyte solutions and distinct redox peaks were seen for each salt, cyclic voltammetry was employed. Since various selective peaks appeared upon application, a gold-working electrode was used for this study. The various scan rates were examined both with and without succinic acid. The study used salt alone. Utilizing a gold 18-Karat working electrode impacted by an Au metal electrode, the catalytic oxidation of succinic acid was investigated. Based on cyclic voltammetry data, Tafel slopes were applied for cupric chloride salt both alone and in the presence of succinic acid, and a potential mechanism for redox reactions was proposed. The novelty of this work is to use the Tafel plot graphical representation to explain the kinetic and mechanism of electrocatalytic reaction of cupric ions with succinic acid in strong electrolyte NaCl.

Keywords: Cyclic voltammetry, Cupric chloride, Succinic acid, Thermodynamic parameters, Tafel plot.

Introduction

Cyclic voltammetry (CV) is a widely used electrochemical technique that involves the application of a potential waveform to an electrochemical cell and measuring the resulting current. It provides valuable information about the redox behavior, kinetics, and stability of electroactive species in solution (Gomaa, 2012a). Cyclic voltammetry is a technique used in electrochemistry to study the redox properties of a chemical species. It involves applying a potential to an electrochemical cell and measuring the resulting current as the potential is varied in a cyclic manner. The experiment typically involves three main steps: scanning the potential, measuring the current, and plotting the resulting voltammogram. The potential is scanned linearly over a range of values, usually

from a negative to a positive value and then back again. The current is measured at each potential value, providing information about the redox reactions occurring in the cell (Gomaa, 2012b).

Cyclic voltammetry can provide valuable information about various electrochemical processes, such as oxidation-reduction reactions, electron transfer kinetics, and adsorption/desorption phenomena. It can be used to determine parameters such as peak potentials (E_p), peak currents (I_p), and peak shapes, which can be related to the concentration of species involved in the redox reaction (Gomaa & Abou Elleef, 2013). The technique finds applications in various fields including analytical chemistry, material science, biochemistry, and electrocatalysis. It is commonly used for studying electrode processes at solid-liquid interfaces and for characterizing electroactive materials (Badulla et al., 2021; Diab et al., 2022; Gomaa, 2012; Gomaa et al., 2013; Gomaa & Al-Jahdali, 2012).

A common electrochemical method that offers useful insights into a substance's redox behavior is cyclic voltammetry. Applying a potential waveform to an electrochemical cell and measuring the current response are the steps involved. The cyclic voltammetry can be used in the following:

1. Determination of redox potentials: Organic molecules, metal complexes, and biomolecules can all have redox potentials that can be determined using cyclic voltammetry (Abou Elleef et al., 2021). This knowledge is necessary to comprehend their reactivity and electrochemical behavior.
2. Characterization of electrode processes: By studying the kinetics and mechanisms of electrode processes such electron transfer reactions, adsorption/desorption phenomena, and surface reactions, cyclic voltammetry may be utilised to characterise electrode processes. We can learn a lot about these processes by looking at the voltammogram's position and structure (Abd El-Hady et al., 2019).
3. Analysis of electroactive species: Cyclic voltammetry is frequently used to quantify a range of electroactive species at electrode surfaces or in solutions. Compared to other analytical methods, it has benefits such high sensitivity, selectivity, and quick analysis times (Goma et al., 2020).
4. Biosensing applications: The detection and measurement of biomolecules including DNA, proteins, enzymes, and medicines have all been accomplished using cyclic voltammetry in biosensing applications (Fakayode & Nkambule, 2022). Cyclic voltammetry can offer sensitive and specific detection by immobilising these biomolecules on an electrode surface or employing modified electrodes with particular recognition components.
1. 5. Energy storage and conversion: The development and characterization of energy storage and conversion technologies, such as batteries, supercapacitors, and fuel cells, uses cyclic voltammetry (Gomaa et al., 2020). It aids in comprehension of the redox processes at play in these systems and performance optimization (Gomaa et al., 2020b; Wahba et al., 2024).

This work aims to develop an electrochemical sensing method for the estimation of cupric ions in the form of cupric chloride and to investigate the potential effects of succinic acid on the electrochemical behavior of cupric ions.

Experimental

Acetic anhydride, sodium chloride, and cupric chloride were supplied by Sigma-Aldrich. They utilized deionized water. Three electrodes and the DY2000 (USA) device were used to perform cyclic voltammetry measurements. The working electrode (gold electrode), reference electrode (Ag/AgCl/saturated KCl), and auxiliary electrode (Pt electrode) are the various electrodes.

Results and discussion

Cupric ion determination

The 18-karat gold electrode was used as the working electrode for the cyclic voltammetry, which was carried out with a 0.1 M NaCl solution and various concentrations of cupric chloride (0.1 M). There are two significant reduction and oxidation peaks in the window range of 1.0 to 1.5 V where the waves are present when the gold electrode is present. The cathodic and oxidation waves were seen to rise with the addition of various amounts of $CuCl_2$ (0.1 M) (Durmishi et al., 2008).

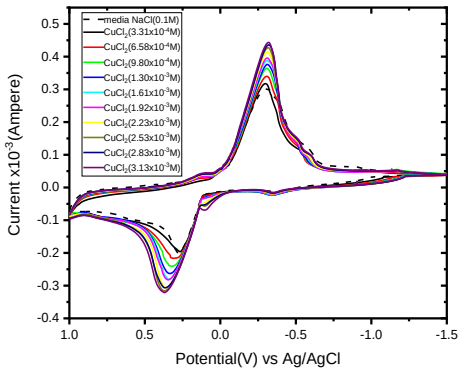

Figure 1. Voltamgraph using different $CuCl_2$ concentrations in NaCl solution as a supporting electrode, scanning at 0.1V/s and in the potential range of 1 to 1.5V at 295 K.

The reduction of divalent copper ions to copper metal is represented by the reduction and oxidation peaks, and the oxidation process results in the reverse oxidation process.

A small oxidation peak was also seen at about -0.1 V, which was attributed to by the gold 18-karat electrode and represented the catalytic hydroxide ion production peak:

$$2H_2O + 2\,e^- \leftrightarrow H_2 + 2\,OH^-$$

Table 1. The kinetic parameters (E_{pa}, E_{pc}, Ip_a, Ip_c, ΔEp, E^o, and $E_{1/2}$) of various concentrations of Cu^{+2} at 295 K and scan rate (0.1 Vs^{-1}).

$[Cu^{+2}]\times10^{-6}$ (mol.cm^{-3})	E_{pa} (Volt)	E_{pc} (Volt)	(-)Ipa$\times10^{-4}$ (Amp)	Ipc$\times10^{-4}$ (Amp)	ΔEp (Volt)	E° (Volt)	$E_{1/2}$ (Volt)
0.662	0.25951	-0.29868	1.67	2.61	0.55819	-0.01959	-0.16537
1.32	0.27745	-0.29925	1.81	2.94	0.57670	-0.01090	-0.16587
1.96	0.29720	-0.29925	1.98	3.15	0.59644	-0.00103	-0.16587
2.60	0.32114	-0.29925	2.23	3.28	0.62038	0.01094	-0.16382
3.23	0.32729	-0.31247	2.27	3.40	0.63977	0.00741	-0.16857
3.85	0.34576	-0.29925	2.25	3.46	0.64501	0.02326	-0.16518
4.46	0.34576	-0.29925	2.26	3.67	0.64501	0.02326	-0.16587
5.06	0.35807	-0.31772	2.41	3.71	0.67579	0.02018	-0.16382
5.66	0.35192	-0.31772	2.31	3.82	0.66963	0.01710	-0.16860
6.25	0.35807	-0.30540	2.27	3.91	0.66348	0.02633	-0.17202

Table 2. The kinetic parameters (Da, Dc, KsC, Γc, Qc, Γa, and Qa) of various concentrations of Cu^{+2} ions at 295K and scan rate (0.1 Vs^{-1}).

$[Cu^{+2}]\times10^{-6}$ (mol.cm^{-3})	Da$\times10^{-4}$ (cm^2.s^{-1})	Dc$\times10^{-4}$ (cm^2.s^{-1})	ks.10^{-4} (cm.s^{-1})	Γc $\times10^{-8}$ (mol.cm^{-2})	Qc x10^{-4} (C)	Γa $\times10^{-8}$ (mol.cm^{-2})	(-) Qa$\times10^{-4}$ (C)
0.662	11.1	27.2	0.783	2.19066	1.33	1.39803	0.847
1.32	3.33	8.72	0.638	2.46422	1.49	1.52202	0.922
1.96	1.78	4.51	0.676	2.64024	1.60	1.65861	1.00
2.60	1.30	2.80	0.847	2.75758	1.67	1.87525	1.14
3.23	0.869	1.94	1.00	2.85205	1.73	1.90684	1.16
3.85	0.601	1.42	0.982	2.90426	1.76	1.89104	1.15
4.46	0.448	1.18	0.900	3.07802	1.87	1.8933	1.15
5.06	0.397	0.942	1.37	3.11639	1.89	2.02418	1.23
5.66	0.291	0.799	1.13	3.20891	1.94	1.93618	1.17
6.25	0.231	0.687	0.986	3.28563	1.99	1.90684	1.16

$CuCl_2$ cyclic voltammetry in 0.1 M NaCl in the presence of succinic acid:

The impact of varying succinic acid concentrations on $CuCl_2$ cyclic voltammetry was investigated. Figure 2 displays the analyzed cyclic voltammograms.

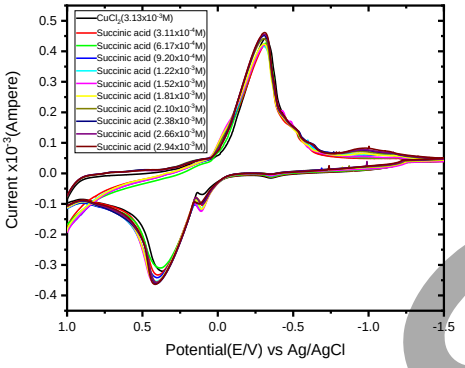

Figure 2. The impact of adding different succinic acid concentrations to $CuCl_2$ (6.25×10^{-3} M) in the potential range of 1 V to -1.5 V at 295 K and scan rate of 0.1 V/s.

The observation of an additional oxidation peak at roughly 0.1 V can be attributed to the catalytic oxidation of succinic acid, which was facilitated by the slow consumption of two electrons by the gold 18-karat electrode, as illustrated in Figure 2.

$$(CH_2\text{-}COOH)_2 \rightarrow (CH_2\text{-}COO)_2^- + 2H^+ + 2e$$

A hydroxyl radical is created when the hydrogen ions interact with the oxygen in the solution. Furthermore, the two stages that show up in the cyclic voltammograms correspond to a step-by-step oxidation of one electron (Olajire & Imeokparia, 2001).

Complexation between $CuCl_2$ and succinic acid is shown by the decrease in all solvation and kinetic parameters with the increase in succinic acid concentration, as shown in Figure 3 and Tables 3 and 4.

Table 3. The kinetic parameters (Epa, Epc, Ipa, Ipc, ΔE_p, E^o, and $E_{1/2}$) of Cu^{+2} ions (6.25×10^{-3} M) with various concentrations of succinic acid at 295 K and scan rate (0.1 Vs^{-1}).

$[Cu^{+2}]\times10^{-6}$ (mol.cm^{-3})	[L]$\times10^{-6}$ (mol.cm^{-3})	Epa (Volt)	Epc (Volt)	(-)Ipa $\times10^{-4}$ (Amp)	Ipc$\times10^{-4}$ (Amp)	ΔE_p (Volt)	E° (Volt)	$E_{1/2}$ (Volt)
0.662	0.621	0.37586	-0.31622	2.54	3.18	0.69208	0.02982	-0.18063
1.32	1.23	0.36423	-0.30646	2.33	3.50	0.67069	0.02888	-0.15839
1.96	1.84	0.38817	-0.29236	2.67	3.33	0.68053	0.04790	-0.15893
2.60	2.44	0.39432	-0.30443	2.76	2.95	0.69875	0.04495	-0.16988
3.23	3.03	0.40664	-0.30970	2.83	2.94	0.71633	0.04847	-0.17437
3.85	3.61	0.40048	-0.30540	2.81	3.05	0.70588	0.04754	-0.16724
4.46	4.19	0.39432	-0.29309	2.86	3.49	0.68742	0.05062	-0.15219
5.06	4.76	0.39432	-0.29925	2.91	3.49	0.69357	0.04754	-0.15994
5.66	5.33	0.38817	-0.29309	2.83	3.64	0.68126	0.04754	-0.15492
6.25	5.88	0.40664	-0.30316	2.91	3.60	0.70980	0.05174	-0.15744

Using a gold 18-karat working electrode, the influence of scan rates was investigated for 6.25×10-3 M of CuCl2 in 0.1 m NaCl solution at 295K. The observed cyclovoltammogram was provided in Figure 3, and the analytical data was found in Tables 5 and 6. Diffusion mechanisms are indicated by a drop-in scan rate, which decreases most data.

The Cu-Succinic acid complex's various cyclic

voltammograms were assessed and examined, yielding the information shown in Tables 7 and 8.

Table 4. The kinetic parameters of Cu^{+2} ions ($6.25x10^{-3}$ M) with various concentrations of succinic acid at 295 K and scan rate ($0.1\ Vs^{-1}$).

$[Cu^{+2}]\times10^{-6}$ (mol.cm^{-3})	[L] $\times10^{-6}$ (mol.cm^{-3})	Da $\times10^{-5}$ (cm^2.s^{-1})	Dc $\times10^{-5}$ (cm^2.s^{-1})	ks.10^{-4} (cm.s^{-1})	$\Gamma c\times10^{-8}$ (mol.cm^{-2})	Qc $\times10^{-4}$ (C)	$\Gamma a\times10^{-8}$ (mol.cm^{-2})	(-)Qa $\times10^{-4}$ (C)
0.662	0.621	2.93	4.59	1.40	2.66938	1.62	2.13072	1.29
1.32	1.23	2.51	5.62	0.975	2.93428	1.78	1.95969	1.19
1.96	1.84	3.31	5.15	1.19	2.79164	1.69	2.23761	1.36
2.60	2.44	3.59	4.09	1.51	2.47225	1.50	2.316	1.40
3.23	3.03	3.83	4.13	2.15	2.47142	1.50	2.37776	1.44
3.85	3.61	3.80	4.50	1.80	2.56304	1.55	2.35638	1.43
4.46	4.19	3.98	5.97	1.43	2.9336	1.78	2.39676	1.45
5.06	4.76	4.18	6.04	1.63	2.9336	1.78	2.43952	1.48
5.66	5.33	4.01	6.62	1.35	3.05237	1.85	2.37776	1.44
6.25	5.88	4.28	6.56	2.29	3.02184	1.83	2.43952	1.48

Impact of varying scan speeds on the redox of $CuCl_2$ in isolation and the Cu-succinic acid intermediate:

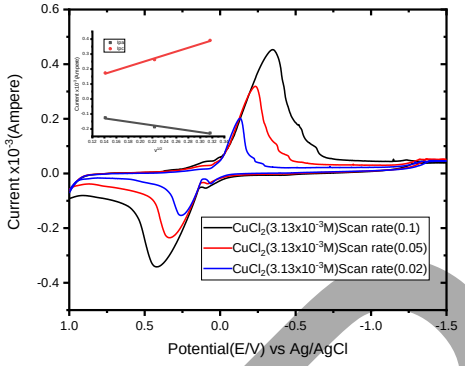

Figure 3. Voltammograms of various scan rates (0.1-0.05-0.02 V/s) of $CuCl_2$ (6.25×10^{-3} M) in the potential range from 1 to -1.5 V at 295 K.

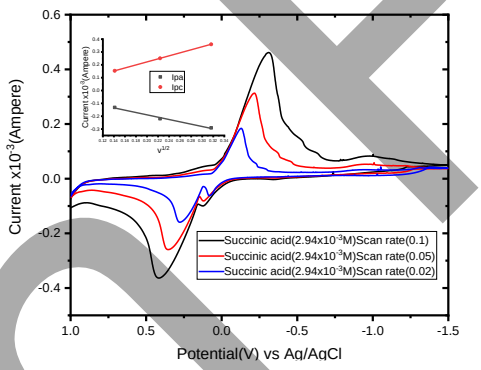

Figure 4. Voltammograms of various scan rates (0.1-0.05-0.02 V/s) of $CuCl_2$ (5.88×10^{-3} M) with succinic acid (5.88×10^{-3} M) in the potential range from 1 to -1.5 V at 295 K.

Table 5. The kinetic parameters of different concentrations of Cu^{+2} at different scan rates (0.1, 0.05, 0.02, and 0.01) Vs^{-1} and at 295 K (Ep_a, Ep_c, Ip_a, Ip_c, ΔE_p, E^o, and $E_{1/2}$).

ν (V.s^{-1})	Ep_a (Volt)	Ep_c (Volt)	(-)$Ip_a\times10^{-4}$ (Amp)	$Ip_c\times10^{-4}$ (Amp)	ΔE_p (Volt)	E^o (Volt)	$E_{1/2}$ (Volt)
0.1	0.35807	-0.30540	2.27	3.91	0.66347	0.02633	-0.17202
0.05	0.31202	-0.22036	1.86	2.63	0.53238	0.04583	-0.11434
0.02	0.24647	-0.12884	1.25	1.74	0.37530	0.05881	-0.05682

Table 6. The kinetic parameters of different Cu^{+2} concentrations at varied scan speeds (0.1, 0.05, 0.02, and 0.01) Vs^{-1} and at 295 K (D_a, D_c, k_s , Γ_c, Q_c, Γ_a, and Q_a)

ν (V.s^{-1})	$D_a\times10^{-4}$ (cm^2.s^{-1})	$D_c\times10^{-4}$ (cm^2.s^{-1})	$k_s\times10^{-4}$ (cm.s^{-1})	$\Gamma_c\times10^{-8}$ (mol.cm^{-2})	$Q_c\times10^{-4}$ (C)	$\Gamma_a\times10^{-8}$ (mol.cm^{-2})	(-) $Q_a\times10^{-4}$ (C)
0.1	0.926	2.75	1.97	3.28563	1.99	1.90684	1.16
0.05	1.24	2.48	0.113	4.41584	2.68	3.12506	1.89
0.02	1.41	2.71	0.0041	7.29442	4.42	5.26504	3.19

Table 7. The kinetic characteristics of Cu^{+2} ions (6.25×10^{-3} M) at different scan speeds (0.1, 0.05, 0.02, and 0.01) Vs^{-1} and at 295 K at varied concentrations of succinic acid (Ep_a, Ep_c, Ip_a, Ip_c, ΔE_p, E^o, and $E_{1/2}$).

ν (V.s^{-1})	Ep_a (Volt)	Ep_c (Volt)	(-)$Ip_a\times10^{-4}$ (Amp)	$Ip_c\times10^{-4}$ (Amp)	ΔE_p (Volt)	E^o (Volt)	$E_{1/2}$ (Volt)
0.1	0.40663	-0.30316	2.91	3.60	0.70980	0.05174	-0.15744
0.05	0.34280	-0.20497	2.20	2.51	0.54777	0.06891	-0.10123
0.02	0.26186	-0.12859	1.31	1.54	0.39045	0.06663	-0.04708

Table 8. The kinetic characteristics (D_a, D_c, KsC, Γ_c, Q_c, Γ_a, and Qa) of Cu^{+2} ions (6.25×10^{-3} M) at varied scan speeds (0.1, 0.05, 0.02, and 0.01) Vs^{-1} and at 295 K with varying concentrations of succinic acid.

ν (V.s^{-1})	$D_a\times10^{-4}$ (cm^2.s^{-1})	$D_c\times10^{-4}$ (cm^2.s^{-1})	$K_s\times10^{-4}$ (cm.s^{-1})	$\Gamma_c\times10^{-8}$ (mol.cm^{-2})	$Q_c\times10^{-4}$ (C)	$\Gamma_a\times10^{-8}$ (mol.cm^{-2})	(-)$Qa\times10^{-4}$ (C)
0.1	1.71	2.62	4.58	3.02184	1.83	2.43952	1.48
0.05	1.96	2.55	0.156	4.21203	2.55	3.68945	2.24
0.02	1.75	2.39	0.0049	6.45392	3.91	5.51327	3.34

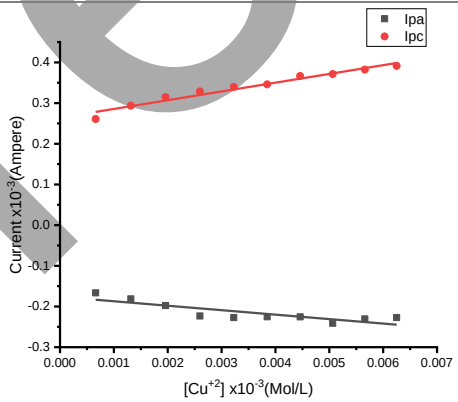

Figure 5. The Relationship between the peak anodic/cathodic current (Ip_a/Ip_c) and the square root of different scan rates (0.1, 0.05, 0.02, and 0.01) Vs^{-1} for Cu^{+2} ions at 295 K.

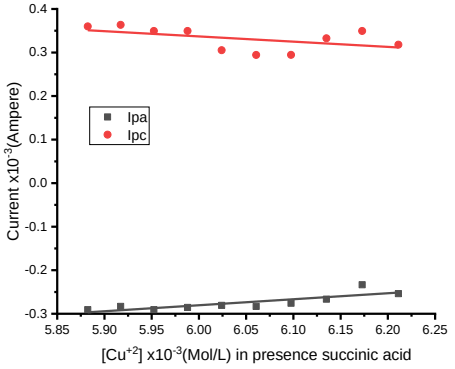

Figure 6. The relation between anodic/cathodic current peak (Ip_a/Ip_c) versus square root of various scan rates (0.1, 0.05, 0.02, and 0.01) Vs^{-1} for Cu^{+2} ions with succinic acid at 295 K.

The quasi-irreversibility is primarily demonstrated by activation using a gold working electrode of the reaction at various scan rates with tiny values of the slopes for the anodic and cathodic waves, as shown in Figs. 5 and 6.

Tafel plot evaluation:

Data appeared when the relationship between overvoltage, measured volt, and the logarithm of peak current in the rising section of the reduction peaks at various $CuCl_2$ concentrations and in the presence of succinic acid was drawn. Beginning with the date that was available, straight lines were plotted; each line's slope and intercept were assessed and shown in the displayed figures. Figure 7 shows several straight plot interactions with the Tafel plots. At low $CuCl_2$ concentrations, the observations are interpreted as follows. According to Tafel plots, a diffusion-controlled reaction is indicated by points that lie on a straight line with a large Tafel slope (El-Baz & Abbas, 2017; El-Kot et al., 2023; Gruden et al., 2014; Mohamed et al., 2020; Ye & Crooks, 2005). Because of the association processes between the molecules ($CuCl_2$-succinic acid) of the employed electrolyte, straight Tafel plots with values for the Tafel plot slopes for $CuCl_2$+succinic acid at different concentrations is obtained (see Figure 8). These Tafel plots are lower than those for diffusion. Tafel plots' final behavior could be explained by a regulated mixture of activation and diffusion mechanisms.

Table 9. Tafel slope, transfer coefficient, and exchange current density of different concentration of Cu^{+2} in 0.1 M NaCl

$[Cu^{+2}]$ (Mole/L)	Slope	α	LOG (i_o)	i_o x10^{-5}(Amp)
6.62×10^{-4}	-4.8479	0.7165	-4.1411	7.23
1.32×10^{-3}	-4.0882	0.9052	-4.1053	7.85
1.96×10^{-3}	-4.0439	0.9062	-4.0456	9.00
2.60×10^{-3}	-3.7806	0.9124	-4.0999	7.95
3.23×10^{-3}	-3.0185	0.9300	-4.176	6.67
3.85×10^{-3}	-3.1271	0.9275	-4.1659	6.82
4.46×10^{-3}	-3.0163	0.9301	-4.1441	7.18
4.12×10^{-3}	-2.9055	0.9326	-4.1236	7.52
5.66×10^{-3}	-2.5965	0.9398	-4.1468	7.13
6.25×10^{-3}	-2.8327	0.9343	-4.0933	8.07

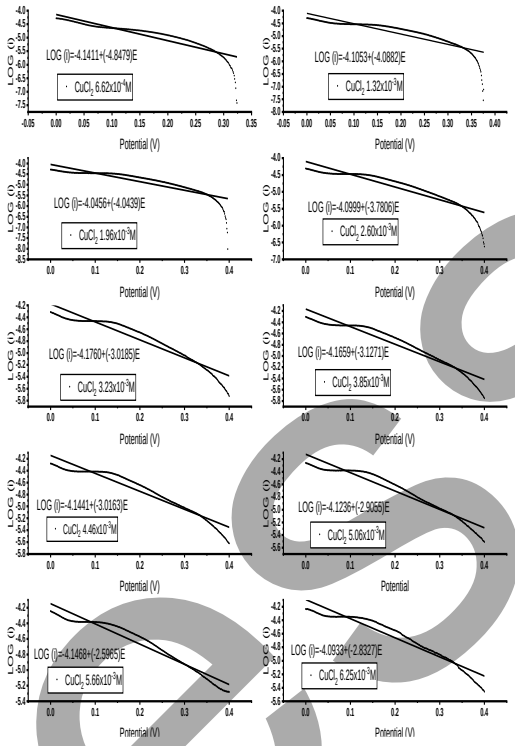

Figure 7. Tafel plot of different concentrations of $CuCl_2$ alone in NaCl medium.

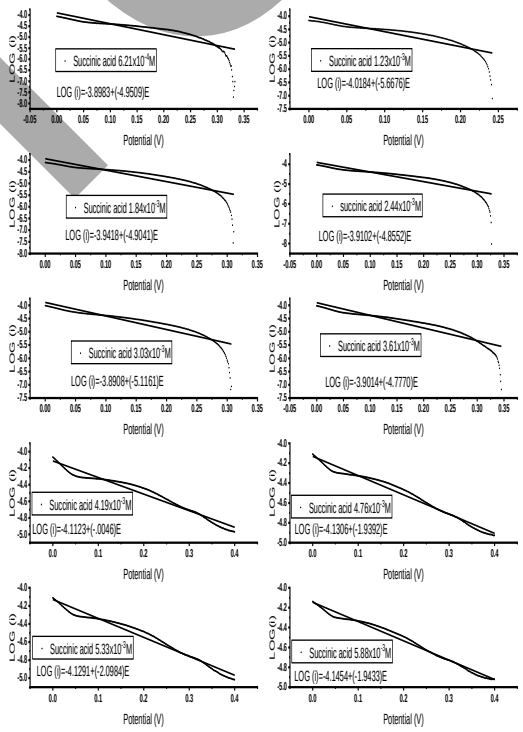

Figure 8. Tafel plot of the effect of different concentrations of succinic acid on $CuCl_2$ in NaCl medium.

Table 10. Tafel slope, transfer coefficient, and exchange current density of different concentration of succinic acid in 6.25×10^{-3} M $CuCl_2$

[Succinic acid] (Mole/L)	Slope	α	LOG (i_o)	i_o x10^{-5}(Amp)
6.21×10^{-4}	-4.9509	0.8851	-3.8983	12.6
1.23×10^{-3}	-5.6676	0.8686	-4.0184	9.59
1.84×10^{-3}	-4.9041	0.8863	-3.9418	11.4
2.44×10^{-3}	-4.8552	0.8874	-3.9102	12.3
3.03×10^{-3}	-5.1161	0.8813	-3.8908	12.9
3.61×10^{-3}	-4.777	0.8892	-3.9014	12.5
4.19×10^{-3}	-2.0046	0.9535	-4.1123	7.72
4.76×10^{-3}	-1.9392	0.9550	-4.1306	7.40
5.33×10^{-3}	-2.0984	0.9513	-4.1291	7.43
5.88×10^{-3}	-1.9433	0.9549	-4.1454	7.15

A good straight line with a large Tafel plot slope supporting the diffusion mechanism reaction was obtained by applying the Tafel plot relation for the complex formed by the interaction between $CuCl_2$ and succinic acid (Figure 9). Slopes smaller than those of $CuCl_2$ alone proved the complexation reaction.

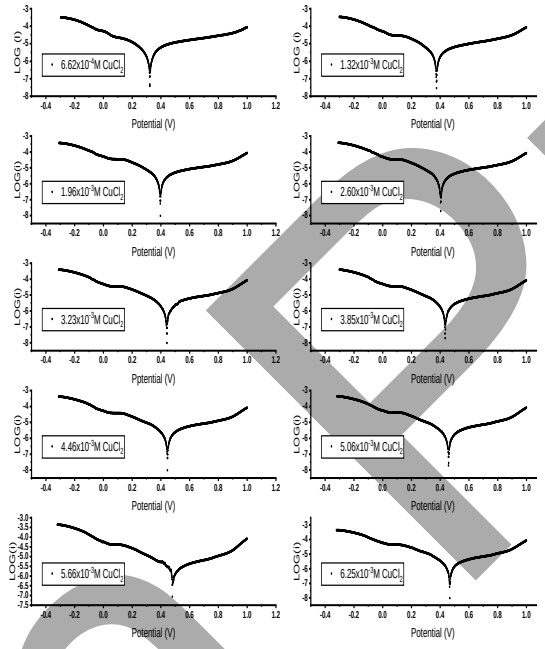

Figure 9. Tafel volt polarization for $CuCl_2$ alone in 0.1 M NaCl

The relationship between the electrode potential and the associated current density during an electrochemical reaction is represented graphically by the Tafel diagram. Its sole purpose is to ascertain the reaction mechanism and examine the kinetics of electrode reactions. Data from the Tafel plot for $CuCl_2$ solvation in 0.1 M NaCl solution. Two straight lines with varying intercepts and slopes are displayed in the plot. The more negative the s1ope, the fastter the reduction procss ocurs. The intercept represents the e1ectrode potentia1 at zero current densitty. In comp1exation between $CuCl_2$ a1one and succinic acid (Figure 10).

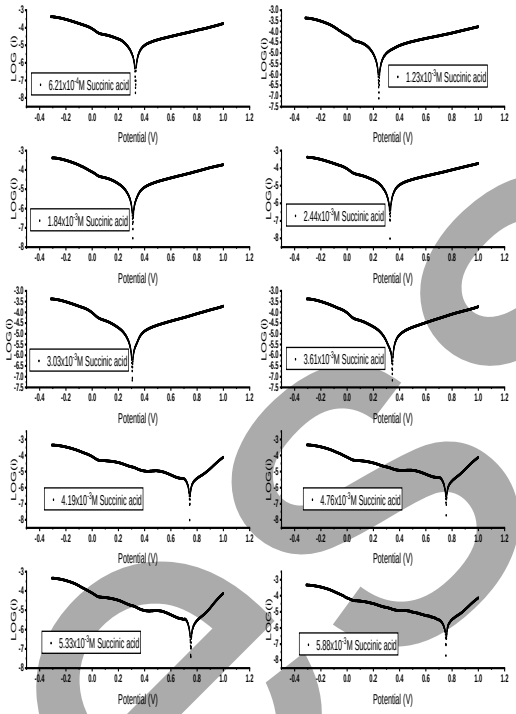

Figure 10. Tafel volt polarization for $CuCl_2$ with succinic acid in 0.1 M NaCl.

Tafel volt polarization:

Tafel polarization describes the relationship between the current density and potential in an electrochemical reaction, while Tafel volt polarization refers to the electrode potential deviation from the equilibrium potential caused by Tafel's behavior. On drawing the Tafel plots for the volt change in the range from -0.4 V to 1.1 V, curves with three different parts are obtained for $CuCl_2$ alone and $CuCl_2$ with succinic acid, as given in Figures 9, and 10, The first line on the left side is responsible for electron transfer, followed by the second line on the left for mass electro-reduction following diffusion control. The third line on the right side is responsible for the precipitation beginning. The meeting between the second and third lines is the Tafel volt polarization. The Tafel plot polarization shifts to the right side by increasing in both $CuCl_2$ alone, $CuCl_2$ + succinic acid concentrations, indicating an increase in diffusibility in case of $CuCl_2$ alone and increase in association, complexation in case of $CuCl_2$ + succinic acid reactions.

Gibbs free energy:

The Gibbs free energy of the cupric chloride and succinic acid interaction in 0.1 M NaCl:

Following the cited references (AbouElleef et al., 2021; Babg et al., 2022; Daud et al., 2013; Gomaa et al., 2017; Gomaa et al., 2018; Kayali e al., 2022; Mohamed et al., 2023; Murray et al., 1998; Nakanishi et al., 2020; Rossotti et al., 1961; Sharfalddin et al., 2021; Shinagawa et al., 2015; Yin et al., 2021), the stability constants and Gibbs free energies of the interaction between cupric chloride and succinic acid were calculated. The resulting values, which vary depending on the chemical and physical processes, are displayed in Tables 11 and 12.

Table 11. Thermodynamic data of Cu-succinic complex at 295 K.

$Cu^{+2}]\times10^{-}$ (mol.cm^{-3})	$[L]\times10^{-6}$ mol.cm^{-3}	(Ep_a),M (Volt)	(Ep_a),L (Volt)	(-)ΔG (KJ/mole)	Log [L]	Log (Bj)
6.21	0.621	0.0263	0.0298	2.8357	-6.2068	0.5017
5.92	5.33	0.0263	0.0475	22.7308	-5.2736	4.0222
5.88	5.88	0.0263	0.0517	24.6568	-5.2304	4.3630
6.10	2.44	0.0263	0.0449	9.0961	-5.6127	1.6095
6.06	3.03	0.0263	0.0484	11.321	-5.5185	2.0034
6.02	3.61	0.0263	0.0475	14.3606	-5.4419	2.5411
6.13	1.84	0.0263	0.0479	5.5607	-5.7350	0.9839
5.95	4.76	0.0263	0.0475	19.9701	-5.3222	3.5337
6.17	1.23	0.0263	0.0288	6.1861	-5.9084	1.0946
5.99	4.19	0.0263	0.0506	16.5876	-5.3776	2.9351

Table 12. Thermodynamic data of Cu-succinic complex at 295 K at mole ratio (1:1).

$[Cu^{+2}]\times10^{-6}$ (mol.cm^{-3})	$[L]\times10^{-6}$ (mol.cm^{-3})	(Epa),M (Volt)	(Epa),L (Volt)	(-)ΔG (KJ/mole)	Log[L]	Log(Bj)
5.88	5.88	0.0263	0.05173609	24.6568	-5.2304	4.3630
5.88	5.88	0.0458	0.06891245	25.1040	-5.2304	4.4421
5.88	5.88	0.0588	0.06663247	28.0500	-5.2304	4.9634

Conclusions

A gold 18-karat working electrode is used in this study's cyclic voltammetry to estimate cupric ions, which is a follow-up to previous research. Sharp peaks arise for any concentration of cupric ions, and the intensities of these peaks increase with the concentration of cupric ions. Evaluation and discussion of the kinetic, solvation, and thermodynamic characteristics were conducted while examining the impact of varying amounts of succinic acid employed as a ligand. In order to visualize reduction potentials, Tafel plots are created on the increasing logarithm of current and overvoltage; several straight lines were produced. Plots of Tafel were used to assess the slopes, and activation or diffusion was proposed as the electrochemical mechanism depending on the situation.

Declaration of interests

The authors declare that they have no conflicts with anybody about this work.

Highlights:

Using a gold electrode (18-karat), cyclic voltammetry can easily estimate copper ions quantitatively. The stability constants and Gibbs free energies for interaction of cupric ions with succinic acid were estimated.

References

Abd El-Hady MN, Gomaa EA, Al-Harazie AG. 2019. Cyclic voltammetry of bulk and nano CdCl2 with ceftazidime drug and some DFT calculations. *J. Mol. Liq*., 276, 970-985.

AbouElleef EM, Abd El-Hady MN, Gomaa EA, Al-Harazie AG. 2021. Conductometric association parameters for $CdBr_2$ in the presence and absence of Ceftazidime in water and 30% ethanol--water mixtures. *J. Chem. Eng. Data*., 66, 878–889.

Almeida JMS, Dornellas RM, Yotsumoto-Neto S, Ghisi M, Furtado JGC, Marques EP, Aucélio RQ, Marques ALB. 2014. A simple electroanalytical procedure for the determination of calcium in biodiesel. *Fuel*., 115, 658–665.

Babg BA, Alzaidi NA, Alsayari JH, Emwas AHM, Jaremko M, Abdellattif MH, Aljahdali M, Hussien MA. 2022. Synthesis, HSA-Binding and Anticancer Properties of $[Cu^2$ dppm$)^2(N\hat{}\ N)_2]^{2+}$. *J. Inorg. Organomet. Polym. Mater*., 32, 4005–4013.

Badulla WFS, Hussein WA, Weiam AA, Arli G. 2021. Study of electrochemical behavior of two chemically similar acridines: tacrine and 9-aminoacridine on hanging mercury drop. *Bull. Chem. Soc. Ethiop*., 35(3), 639-646.

Daud N, Yusof NA, Nor SMM. 2013. Electrochemical characteristic of biotinyl somatostatin-14/Nafion modified gold electrode in development of sensor for determination of Hg (II). *Int. J. Electrochem. Sci*., 8, 10086–10099.

Diab MA, El-Sonbati AZ, Gomaa EA, El-Mogazy

MA, Morgan ShM, Abou-Dobara MI, Omar NF, El-Zahed MM, Osman1 MA. 2022. Polymer complexes: LXXIX—synthesis, characterization, geometrical structures, biological activity and molecular docking studies of azo dye complexes. *J. Iran Chem. Soc*., 19(7), 3079–3102.

Durmishi BH, Ismaili M, Shabani A, Jusufi S, Fejzuli X, Kostovska M, Abduli S. 2008. The physical, physical-chemical and chemical parameters determination of river water Shkumbini (Pena)(part A). *Ohrid, Repub. Maced.*, 27, 1–11.

El-Baz AF, Abbas HM. 2017. Isolation and identification of an endophytic fungus from ficus elastica decora and investigation of the antioxidant and antifungal bioactivities of its fermentation extract. *Menoufia J. Agric. Biotechnol*., 2, 81–85.

El-Kot DA, Gomaa EA, El-Askalany AH, Zaky RR, Abd El-Hady MN. 2023. Design of a novel-NOON-tetradentate Schiff-base scaffold supported by $α$-tetralone and benzothiazole moieties with its Cu^{2+}, Co^{2+}, and Cd^{2+} chelates. *J. Mol. Struct*., 1, 134901.

Fakayode OJ, Nkambule TTI. 2022. Cyclic voltammetric determination of calcium in water in the presence of natural organic matter (humic acid) and Cu (II) at gold electrode's surface. *Food Chem. Adv*., 1, 100012.

Gomaa EA. 2012a. Gibbs free energies, enthalpies and entropies of transfer for reference ions Ph4As+ and Ph4B- in mixed DMFA-H_2O solvents at different temperatures. *Am. J. Environ. Eng.*, 2, 54-57.

Gomaa EA. 2012b. Molal solubility, dissociation, association and solvation parameters for saturated benzoic acid solutions in various solvents at 298.15 K. *Phys. Chem. Liq.*, 50, 279-283.

Gomaa EA. 2012c. Molal solubility, dissociation, association and solvation parameters for saturated phenylalanine solutions in various solvents at 298.15 K. *Am. J. Biochem*., 2, 25-28.

Gomaa EA, Al-Jahdali BA. 2012. Conductometric studies of calcium ions with kryptofix 221 in mixed MeOH-DMF solvents at different temperatures. *Education.*, 2, 37-40.

Gomaa EA, Abou Elleef EM, Abdel-Razek MG. 2013. Thermodynamics of the solvation of CaSO4 in mixed DMF-H2O at 301.15 K. *Int. Res. J. Pure Appl. Chem.*, 3, 320-325.

Gomaa EA, Abou Elleef EM. 2013. Thermodynamics of the solvation of potassium thiocyanate in mixed EtOH-H_2O solvents at 301.15 K. *Sci. Technol*., 3, 118-122.

Gomaa EA, Tahoon MA, Negm N. 2017a. Aqueous micro-solvation of Li^+ ions: Thermodynamics and energetic studies of Li^+-(H_2O) n (n= 1--6) structures. *J. Mol. Liq*., 241, 595–602.

Gomaa EA, Zaky RR, Shokr A. 2017b. Estimated the physical parameters of lanthanum chloride in water-N, N-dimethyl formamide mixtures using different techniques. *J. Mol. Liq*., 242, 913–918.

Gomaa EA, Mahmoud MH, Mousa MG, El-Dahshan EM. 2018. Cyclic voltammetry for the interaction between bismuth nitrate and methyl red in potassium nitrate solutions. *Chem. Methodol*., 3, 1–11.

Gomaa EA, EL-Sonbati AZ, Diab MA, EL-Ghareib MS, Salam HM. 2020a. Cyclic voltammetry, kinetics, thermodynamic and molecular docking parameters for the interaction of nickel chloride with diphenylthiocarbazone. *Open Acad. J. Adv. Sci. Tech*., 4, 30-44.

Gomaa EA, EL-Sonbati AZ, Diab MA, EL-Ghareib MS, Salama HM. 2020b. Voltammetric solvation study for the interaction of $CuBr_2$ with oxalic acid in KBr solution at 18ºC using glassy carbon electrode. *Open Acad. J. Adv. Sci. Tech.*, 4, 15-29.

Goma EA, El-Defraway MM, Hussien SQ. 2020c. Estimation of cyclic voltammetry data for $SrCl_2$, $CaCl_2$ and their interaction with ceftriaxone sodium salt in KNO_3 using palladium working electrode. *Eur. J. Adv. Chem. Res*. 1, 1-6.

Gruden R, Buchholz A, Kanoun O. 2014. Electrochemical analysis of water and suds by impedance spectroscopy and cyclic voltammetry. *J. Sensors Sens. Syst*., 3, 133–140.

Kayali D, Shama NA, Asir S, Dimililer K. 2023. Machine learning-based models for the qualitative classification of potassium ferrocyanide using electrochemical methods. *J. Supercomput*., 79(11), 12472-12491.

Mohamed A, Yousef S, Nasser WS, Osman TA, Knebel A, Sánchez EPZ, Hashem T. 2020. Rapid photocatalytic degradation of phenol from water using composite nanofibers under UV. *Environ. Sci. Eur*., 32, 1–8.

Mohamed F, Gomaa EA, Salem SE, Killa HM, Gouda AA, Farouk AH. 2023. Parameters for the concductometric association for lump and nano $CoSO_4.7H_2O$ in the presence and absence of fuchsin acid in water at different temperatures. *Bull. Chem. Soc. Ethiop*., 37(3), 789-804.

Murray MD, Loos B, Tu W, Eckert GJ, Zhou X-H, Tierney WM. 1998 Effects of computer-based prescribing on pharmacist work patterns. *J. Am. Med. Informatics Assoc*., 5, 546–553.

Nakanishi J, Kuramoto I, Baba J, Ogawa K, Yoshikawa Y, Ishiguro H. 2020. Continuous hospitality with social robots at a hotel. *SN Appl. Sci*., 2, 1–13.

Olajire AA, Imeokparia FE. 2001. Water quality

assessment of Osun River: studies on inorganic nutrients. *Environ. Monit. Assess*., 69, 17–28.

Rossotti FJR, Rossotti H. 1961. The determination of stability constants: and other equilibrium constants in solution. *McGraw-Hill*, 2, 500–584.

Sharfalddin AA, Emwas AH, Jaremko M, Hussien MA. 2021. Synthesis and theoretical calculations of metal-antibiotic chelation with thiamphenicol: in vitro DNA and HSA binding, molecular docking, and cytotoxicity studies. *New J. Chem.*, 45, 9598–9613.

Shinagawa T, Garcia-Esparza AT, Takanabe K. 2015. Insight on Tafel slopes from a microkinetic analysis of aqueous electrocatalysis for energy conversion, *Sci. Rep*., 1-21.

Wahba RH, El-Sonbati AZ, Diab MA, Gomaa EA, AbouElleef EM. 2024. Electrochemical sensing ions cyclic vo;tammetry and investigation of rosemary extract's effects on their behavior: Antibacterial prop[erties of rosmery extract and molecular docking analysis for potential COVID-19 therapeutic benefits. *Microchem. J*., 200, 110398.

Ye H, Crooks RM. 2005. Electrocatalytic O_2 reduction at glassy carbon electrodes modified with dendrimer-encapsulated Pt nanoparticles. *J. Am. Chem. Soc.* 127, 4930–4934.

Yin Q, Xu Z, Lian T, Musaev DG, Hill CL, Geletii YV. 2021. Tafel slope analyses for homogeneous catalytic reactions. *Catalysts*, 11, 87-95.

الملخص العربي

عنوان البحث: معاملات الديناميكية الحرارية لتفاعل كلوريد النحاس مع حمض السكسينيك في محلول كلوريد الصوديوم باستخدام الفولتميتر الدائري

آية فؤاد[١]، عادل زكي السنباطي[١]، مصطفى دياب*[١]، مروة الصياد[٢]، عصام جمعة

[١]قسم الكيمياء، كلية العلوم، جامعة دمياط، دمياط ، مصر.
[٢] قسم طب العيون، كلية الطب، جامعة المنصورة، مصر.
[٣] قسم الكيمياء، كلية العلوم، جامعة المنصورة، الدقهلية، مصر.

تم تعيين تركيزات أيونات النحاس الثنائي باستخدام الفولتامتري الدائري باستخدام الكترود الذهب عيار ١٨ قيراط ومحلول كلوريد الصوديوم كالكترولبت في وجود وفي عدم وجود حمض السكسينيك كمرتبط. ولقد استخدمت منحنيات تافل لدراسة ميكانيكية تفاعل أيونات النحاس الثنائي مع حمض السكسينيك وتم دراسة قمم الأكسدة الاختزال الناتجة من هذه التفاعلات باستخدام الفولتامتري الدائري.